Organic Electronics 59 (2018) 190–195

Contents lists available at ScienceDirect

Organic Electronics

journal homepage: www.elsevier.com/locate/orgel

Letter

Effect of the vapor diffusion and improved light harvesting for Perovskite-Cu_2ZnSnS_4 hybridized solar cells

Shih-Jen Lin[a], Jyh-Ming Ting[a,*], Chia-Tsung Hung[b], Yaw-Shyan Fu[b,**]

[a] *Department of Materials Science and Engineering, National Cheng Kung University, Tainan 701, Taiwan, ROC*
[b] *Department of Greenergy, National University of Tainan, Tainan 700, Taiwan, ROC*

ARTICLE INFO

Keywords:
Perovskites
Cu_2ZnSnS_4 (CZTS)
Grain growth
Grain boundaries

ABSTRACT

In this study, a novel hybridized perovskite-Cu_2ZnSnS_4 solar cell has been demonstrated. The $CH_3NH_3PbI_3$ layer was synthesized using a facile one-step solution process under ambient conditions. The precursor solution consists of an equimolar methylammonium ion [MA^+] and [PbI_3^-] anion in heptane solvent. The vapor-assisted crystal growth at the grain boundaries occur due to the methylamine (CH_3NH_2, MA). Moreover, 1 wt% Cu_2ZnSnS_4 (CZTS) nanoparticles (NPs) was added to the solution to enhance not only the absorption from visible to infrared regions and but also the transfer of the photogenerated charge carriers, leading to reduced charge recombination. The device structure was glass/ITO/1 wt% CZTS NPs hybrid poly (3,4-ethylenedioxythiophene) poly (styrene-sulfonate) (PEDOT:PSS)/$CH_3NH_3PbI_3$ ($MAPbI_3$)/C60/BCP/Al. The obtained $MAPbI_3$ perovskite-based solar cell shows a short-circuit current density of 19.00 mA/cm^2, an open-circuit voltage of 0.84 V, a fill factor of 0.47, and a power conversion efficiency (PCE) of 7.55%.

1. Introduction

In recent years, inorganic – organic perovskite solar cells have been highly considered due to their long electron-hole diffusion lengths, low temperatures processing, and outstanding photoelectric properties [1–3]. Organic halide perovskites have ABX_3 crystal structures (A = organic cation, alkali; B = Ge, Sn, Pb and X = halide), where the band gap can be adjusted through varying material compositions. The typical $CH_3NH_3PbI_3$, $CH_3NH_3PbBr_3$, $CH_3NH_3PbCl_3$, $CH_3NH_3PbI_{3\text{-}x}Cl_x$, $CH_3NH_3PbBr_{3\text{-}x}Cl_x$, and $CH_3NH_3PbBr_{3\text{-}x}I_x$ Perovskites have been extensively investigated in the field of photodetectors [4–6]. In 2009, Miyasaka's group used $MAPbI_3$ perovskites for dye-sensitized solar cells for the first time [7]. Recent reports have shown higher efficiencies for various device structures. Both single and multiple solution processes have been developed, including solid-state structures with n-i-p mesoscopic TiO_2 [8,9], super-meso structures Al_2O_3 scaffold [10], and nickel oxide-based structures with a p-i-n planar heterojunction (PHJ) architecture [11–13]. Furthermore, through a vapor-assisted solution-process deposition technique, in-situ chemical vapor deposition enables a flatter morphology and improved grain size via gas-solid crystallization [14,15]. Lv's et al. employed ternary $CuInS_2$ QDs as a hole transport materials (HTM), where their results strongly suggested that a wide band gap of metal chalcogenide HTM is more efficient with regard to achieving a high open circuit voltage (Voc) [16]. These various types of metal chalcogenide thin film solar cells based on the copper-chalcopyrite family of semiconductors: $CuIn_{1-x}GaxSe_2$ (CIGS), Cu_2ZnSnS_4 (CZTS), and $Cu_2ZnSnSe_4$ (CZTSe). Among them, CZTS is the most appropriate for thin film solar cells because non-toxic, earth-abundant, and inexpensive. Moreover, CZTS also has a high absorption coefficient greater than 10^{-4} cm^2, which making it suitable as a solar-cell absorber. Many studies have shown improvement photocatalytic performance of the open-circuit voltage of solar cell by adjusting the band gap and recombination rate [17,18]. As an example, outstanding open circuit voltage of 1.353 V via a tandem device architecture has been achieved [19]. However, perovskite materials are unstable in polar solvents. Thus, providing more stable constituents of HTM for perovskite-based photovoltaics is needed [20]. Pérez-Prieto et al. reported the highly dispersible and photostable lead perovskite-octadecylammonium bromide (P_{ODA}) by using both toluene and (dimethylformamide) DMF [21]. The perovskite could stable both in colloidal solution in toluene and solid in DMF + toluene. On the other hand, Oleh Vybornyi et al. synthesized perovskite nanocrystal (NCs) with replacing DMF using 1-octadecene (ODE) with the presence of oleylamine and oleic acidv [22]. Therefore, herein, we report high crystalline $MAPbI_3$ films prepared by a one-step methylamine (MA) vapor-assisted solution-precipitation process with polar-free solvents.

---

[*] Corresponding author.
[**] Corresponding author.
E-mail addresses: jting@mail.ncku.edu.tw (J.-M. Ting), ysfu@mail.nutn.edu.tw (Y.-S. Fu).

https://doi.org/10.1016/j.orgel.2018.05.010
Received 17 April 2018; Received in revised form 8 May 2018; Accepted 8 May 2018

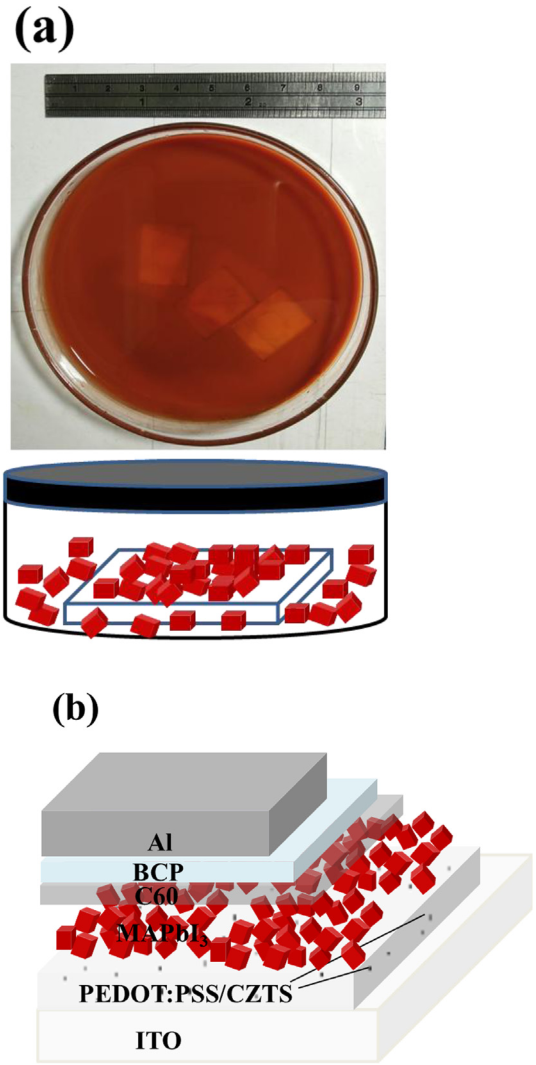

Fig. 1. Schematic illustration of (a) $MAPbI_3$ was synthesized in glass petri dish 9.5 cm in diameter; and, (b) the basic device architecture of the glass/ITO/1 wt % Cu_2ZnSnS_4 hybrid PEDOT:PSS/ $MAPbI_3$ with MA vapor-assisted treatment/ C60/BCP/Al layers.

We demonstrated that MA vapor-enhanced grains growth and crystal size. Moreover, the addition of CZTS NPs hybrid with PEDOT:PSS has been demonstrated to not only form p-type HTM but also broadened the infrared region for a PHJ perovskite device.

2. Materials and methods

2.1. Materials and preparation of the MA^+, PbI_3^- precursors

All chemicals were of analytical grade and used as received without further purification. The methylamine vapor was obtained from methylamine solution (CH_3NH_2, SHOWA, 40%). The vapor was distilled in vacuum condition at 40 °C and injected into oleic Acid (OA, SHOWA, 90%) to form an anhydrous vapor-liquid salt as an $[MA^+][OA^-]$ precursor. The Lead (II) Iodide (PbI_2, SHOWA, 98%) was dispersed in 1-Octadecene (ODE, Acros, 90%) and stirred for 30 min at 150 °C, after which it was purified in a vacuum oven at 100 °C to remove moisture. Finally, oleylamine (OAm, across, approximate C18-content 80–90%) with OA as the surfactant was poured into the mixture until PbI_2 dissolved completely to form a transparent precursor $[PbI_3^-][OAm^+]$.

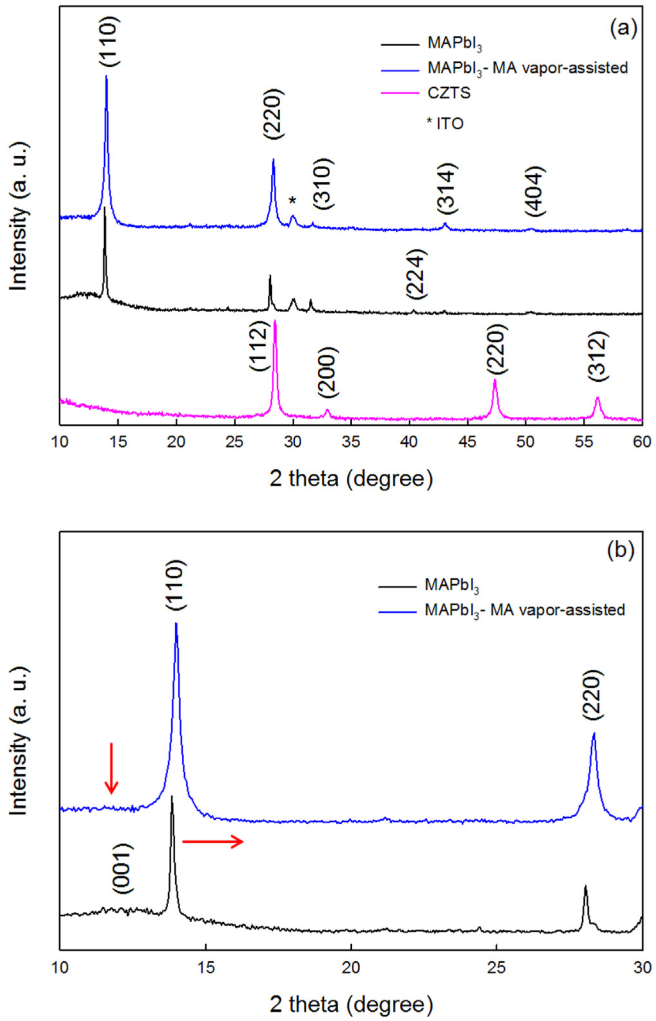

Fig. 2. XRD patterns of as-synthesized (a) kesterite CZTS NPs, tetragonal $MAPbI_3$ NCs with and without MA vapor-assisted treatment, (b) peaks right shift through MA vapor treatment.

2.2. Synthesis of $MAPbI_3$ NCs

$MAPbI_3$ was synthesized by mixing 3 mL 0.1 M MA^+ precursor which was diluted with n-Heptane (C-ECHO, > 99%) and 1 mL 0.1 M PbI_3^-. Meanwhile, the rubyred $CH_3NH_3PbI_3$ NCs were precipitated from the reaction in Fig. 1(a).

2.3. Synthesis of Cu_2ZnSnS_4 NPs

The CZTS NPs were fabricated via a conventional hydrothermal synthesis method as reported in our previous work [23]. Briefly, a certain amount of thiourea (NH_2CSNH_2, Riedel-de Haën, 99%) was dissolved in DI-water. Subsequently, zinc chloride ($ZnCl_2$, Merck, 98%), stannous chloride dehydrate ($SnCl_2{\cdot}2H_2O$, Shimakyu, 98%), and drop of the diethylenediamine ($C_4H_{13}N_3$, Panerac quimica sa, 98%) as chelating regent, finally copper (II) chloride anhydrous ($CuCl_2$, Choneye pure chemicals Co., Ltd., 98%) were added in the solution. The obtained mixture was then transferred in to autoclave and the temperature was set at 180 °C for 72 h.

2.4. Device system

The obtained active area is 0.06 cm^2 of pre-patterned glass/indium-tin-oxide (ITO) (15Ω/sq) was sequentially cleaned with detergent, distilled water, acetone and isopropyl alcohol 30 min, respectively by